

Optimization of hydrogen peroxide/NiO nanoparticle photocatalytic process by degrading cephalixin from aqueous solution using Taguchi method: mineralization, mechanism and pathway

Fateme Asadi^a, Ghorban Asgari^b, Abdolmotaleb Seid-Mohammadi^{b,*}, Zahra Torkshavand^c

^aStudent Research Committee, Department of Environmental Health Engineering, Hamadan University of Medical Sciences, Hamadan, Iran, email: F_asadi56@yahoo.com (F. Asadi)

^bSocial Determinants of Health Research Center, Department of Environmental Health Engineering, Hamadan University of Medical Sciences, Hamadan, Iran, email: sidmohammadi@umsha.ac.ir (A. Seid-Mohammadi), asgari@umsha.ac.ir (G. Asgari)

^cDepartment of Environmental Health Engineering, Hamadan University of Medical Sciences, Hamadan, Iran, email: Zahratorkshavand@yahoo.com (Z. Torkshavand)

Received 7 November 2019; Accepted 3 April 2020

ABSTRACT

The present work investigated the efficiency of nickel oxide nanoparticle (NiO) activated hydrogen peroxide (H₂O₂) in the presence of ultraviolet (UV) irradiation degrading cephalixin (CLX) from aqueous solutions. The effect of pH of the solution (3–9), NiO dosage (1.5–2 mg/L), hydrogen peroxide concentration (5–20 ml/L), contact time (10–60 min) and CLX initial concentration (20–80 mg/L) was studied and optimized using Taguchi design. The percentage contribution of each operational parameter on CLX degradation determined using the analysis of variance. The results showed that in the optimum conditions, an initial concentration of 20 mg/L at pH = 3, 1.5 mg/L of NiO, 10 ml/L hydrogen peroxide with UV irradiation limit after 60 min contact time, degrading of CLX was 99.3%, and the least effective parameter was CLX initial concentration (73.3%). Results for 10 ml/L H₂O₂ in deionized water included a reduction to below the chemical oxygen demand (COD) detection after 60 min with the addition of 20 g/L Na₂CO₃ concentrated solution. Under optimum operational conditions, the rates of CLX mineralization for COD and total organic carbon removal were 83% and 68% within 60 min contact time, respectively. In addition, the removal process of CLX could be described by the pseudo-first-order kinetic model. The liquid chromatography/mass spectrometry was used to selectively detect degradation products of CLX degradation. Also, a tentative pathway for degradation of CLX using the UV/H₂O₂/NiO process was proposed.

Keywords: Photocatalytic degradation; Cephalixin; Hydrogen peroxide; NiO nanoparticle; Taguchi design

1. Introduction

Drugs are natural or synthetic compounds with significant benefits for individuals and the environment. Antibiotics, as a famous pharmaceutical group, are widely used in human medicine. As veterinary drugs, they are used as growth promoters in animal husbandry in livestock and aquaculture operations [1–3]. Based on the antimicrobial

activity, cephalosporins as the most widely used class of antibiotics, are divided into four major groups [1]. Cephalixin (CLX) as the first-generation cephalosporin, is used for the treatment and/or prevention of microbial infections such as respiratory tract, middle ear, skin, bone, and infections, caused by streptococcus bacteria [1,2]. Due to the increased use of antibiotics, these organic compounds are continuously released into the environment

* Corresponding author.

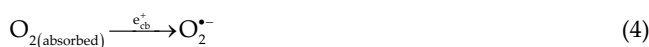
in the range from 0.3 to 200 µg/L and above through various waste streams including urban wastewater treatment plants, households, hospitals, and pharmaceutical companies [1,4]. The increase in antibiotics resistance in different bacteria and genes reduces the therapeutic efficacy of antibiotics against pathogens. This could be the main concern for the release of antibiotics into the environment with a potential risk for aquatic and terrestrial organisms [5]. Therefore, the elimination of antibiotic residues from effluents is important and has generated increasing interest among researchers. Chemical, physical and biological methods such as chemical oxidation [6], biological treatment [7], and membrane techniques [8] have been applied for the removal of antibiotics. Depending on the pollutant concentration in the effluent and the cost of the process, different methods can be adopted. However, due to the low effectiveness of these methods and the inadequacy in their application, it is necessary to develop innovative methods for the effective removal of contaminants from aqueous solutions [9]. Advanced oxidation processes (AOPs) have been successfully applied for treating most of the contaminants in aquatic systems [10]. The reason for the use of AOPs is due to the inability of conventional processes to treat highly contaminated toxic water. In these processes, hydroxyl radicals (HO•) which are involved in mineralization and oxidation of organic compounds to water and carbon dioxide are produced [11]. Free radicals are considered as the strong oxidizing agents which can quickly attack the organic molecules and can separate a hydrogen atom from the organic material structure. In recent years, different AOPs processes such as Fenton and photo-Fenton [12], ozone oxidation [13,14], sonolysis [15], and photocatalytic oxidation [16] have been used for treating a majority of antibiotics compounds in contaminated water. Among AOPs processes, photo-based AOP is an oxidation technology that introduces ultraviolet (UV) irradiation to assist the production and use of hydroxyl radicals as a strong and non-selective oxidant [11]. The use of UV irradiation along with oxidants including hydrogen peroxide [6], ozone [15], and persulfate [6] can be effective in enhancing the function of oxidation processes and increasing the degradation efficiency of organic pollutants. These AOPs have been extensively examined for degradation of different recalcitrant organic compounds through hydroxylation by adding hydroxyl groups to non-saturated bonds) or dehydrogenation. AOPs based hydroxyl radical is a very reactive, non-selective, and powerful oxidizing agent with strong oxidative potential ($E_0 = 2.80$ V). Compared with hydrogen peroxide ($E_0 = 1.76$ V), has been extensively studied for the destruction of a wide range of recalcitrant organics through hydroxylation and/or dehydrogenation. However, the influence of wastewater quality on treatment efficiency is one of the main limitations of this process [17]. The photodegradation of contaminants has been studied by direct absorption of UV irradiation and combined UV/hydrogen peroxide [18–20]. According to the literature, because the use of nanoparticle technology may be a promising approach for degrading organic pollutants, a great deal of attention is focused on the potential of many types of nanomaterials for treating wastewater containing antibiotics. Zerovalent iron nanoparticles have been used for

the removal of antibiotics by applying the Fenton process or other oxidants from aqua solution [21,22]. As effective compounds, copper oxide nanoparticles [23] and zinc oxide [24] have been used for antibiotics removal from polluted water via either adsorption or photodegradation. In this regard, Elmolla and Chaudhuri [25] reported the efficacy of UV/hydrogen peroxide/TiO₂ photocatalysis for the degradation of amoxicillin, ampicillin, and cloxacillin in aqueous solution [25]. Recently, nickel oxide (NiO) nanoparticle, has been studied as a new transition metal activator for removing dyes [26] and antibiotics [27] from wastewater.

NiO nanoparticle [28] are excited to generate positive holes in the valence band ($h\nu_{vb}^+$) with an oxidative potential, as well as negative electrons at the conduction band (e_{cb}^-) with a reductive potential, as Eq. (1) [29]:



These holes and electrons can produce hydroxyl radicals due to the reactions of OH⁻, H₂O, and O₂ at the surface of NiO according to Eqs. (2)–(4):



To the best of our knowledge, the removal of CLX using the integrated approach of UV irradiation, hydrogen peroxide, and NiO has not been investigated so far. The present study investigates the degradation of CLX using a combined approach of UV, hydrogen peroxide, and NiO nanoparticles and surveys the effect of operational parameters including CLX initial concentration, time, pH of the solution, hydrogen peroxide, and NiO concentration and optimization of CLX removal rate using Taguchi orthogonal array (OA) design. One factor at a time method is commonly applied to optimize treatment processes. However, in this technique, it is presumed that operational parameters do not interact with each other and the variable of response is only a function of a single parameter [30]. Recently, optimization methods, such as Taguchi design [31] and response surface methodology [32] have been extensively used in chemistry, different industries, and engineering to obtain the best response. In the Taguchi method, systematic OA is used in the design experiments. In these experiments, the columns corresponding to independent variables are orthogonal to one another. To examine the result of experiments, analysis of variance (ANOVA) and signal-to-noise (S/N) ratio was done, which can identify the involved parameters [31]. In these cases, NiO nanoparticles are easily activated by hydrogen peroxide. The use of UV irradiation with a suitable photocatalyst can reduce apparent activation energy and increase the process efficiency. Evidently, no study has yet performed to investigate the performance of the novel NiO/hydrogen peroxide/UV process using the Taguchi method for determining the required sample size and study on the

degradation mechanism and pathway of CLX in aqueous solution. In the present study, to determine the optimal conditions and evaluate the effects of different parameters on the removal efficiency of CLX, Taguchi design was applied, S/N ratios were measured, and the results were analyzed by ANOVA.

2. Materials and methods

2.1. Materials

Hydrogen peroxide (30% w/w), acetonitrile, ammonium acetate, and CLX (98%) ($C_{16}H_{17}N_3O_4S$), were purchased from Sigma-Aldrich (St. Louis, MO, USA). NaOH and H_2SO_4 were also obtained from Merck Chemical Company, Germany. The NiO nanoparticle (>99% purity, the particle size of 10–20 nm and surface area of 50–100 m^2/g) used in this study was purchased from US Research Nanomaterial's Ltd., Co., USA. All chemicals used were of analytical grade and used without further purification. All solutions were prepared in deionized water that was produced by a Milli-Q Biocel Water System (Germany).

2.2. Photo reactor

This experimental study was done on a laboratory scale in a 1,000 mL pyrex-made reactor, equipped with a turbulent reservoir, a pH meter, and an ultrasonic wave generator. Photo-reactions were carried out in a lab-scale reactor. The schematic diagram of the experimental set-up used in the study is shown in Fig. 1. The reactor was cylindrical with 2.5 L volume and was made from stainless steel. A UV lamp (55 W low-pressure mercury-vapor lamp; radiation flux for degradation 253.7 nm, 156 $\mu W/cm^2$ at 1 m of intensity, Philips Co., Netherlands), immersed in the glass tube, was used for irradiation. The reaction chamber was filled with the reaction mixture, which was placed between the UV lamp and reactor walls.

2.3. Experimental procedure

In this experimental study, CLX removal was achieved in the batch mode by adding hydrogen peroxide as an

oxidant and NiO nanoparticle as a catalyst in the synthetic solution. To prepare a standard solution, 1 g of CLX by double distilled water in the volume of 1,000 cc was prepared. Afterward to provide a 20 mg/L of CLX solution, 1 cc of 1 g/L standard solution with distilled water was prepared in the volume of 1,000 cc. To prepare a 20–80 mg/L solution, the standard solution in 100 volumes was prepared. Briefly, the pH of the CLX sample (1,500 mL) was adjusted to the desired level using NaOH and H_2SO_4 solutions (0.1 mol/L). Afterwards, hydrogen peroxide (5–20 ml/L), NiO nanoparticle (0.5–2 mg/L) and CLX (20–80 mg/L) were added to the stirred solution. The solutions were fed into the photo-reactor in the photocatalytic process. Samples were collected from the reaction vessel at fixed intervals using a 30 mL syringe and pipetted into glass vials. At the end of each experiment, Na_2CO_3 (20 g/L) was added to remove the residue of H_2O_2 to prevent it from interfering, then the sample was shielded to reduce evaporation losses and heated in a water bath at 90°C for a predetermined period of time. Residual H_2O_2 were analyzed at the end of each run by (DR 5000, Hatch, New Zealand) spectrophotometer [33].

2.4. Taguchi OA experimental design

In this study, a L_{16} OA experimental design was used to identify the optimum conditions for the maximum removal of the CLX in a photocatalytic system. This method involves data transformation to a S/N ratio which can indicate the desired value. In other words, the S/N ratio represents the deviation of the mean value and standard deviation for a dataset (“signal” indicates the desirable effect, and “noise” indicates the undesirable effect) [34]. The S/N ratios lower-the-better, nominal-the-best, and higher-the-better ratios and were measured with regard to the higher-the-better characteristic as presented in Eq. (5) [35].

$$\frac{S}{N} = -10 \log_{10} \left[\frac{1}{n} \sum \left(\frac{1}{Y_i} \right)^2 \right] \quad (5)$$

where n represents the number of experiments, and (Y_i) denotes response in each experiment.

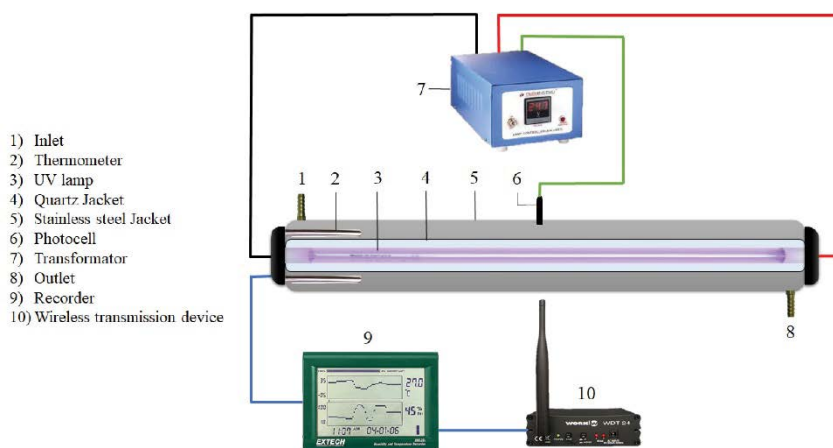


Fig. 1. Schematic diagram of photocatalyst reactor.

In order to determine the optimal condition for the CLX removal using the Taguchi method, different factors such as pH of the solution, hydrogen peroxide concentration, NiO dosage, contact time and initial CLX concentration were selected as the main parameters in four levels to design the experiment. Table 1 presents the OA, levels, and obtained results in Taguchi design. The calculations were performed in Minitab 17 and Design Expert 7 software packages.

2.5. Analysis

After conducting the related experiments, the samples were collected at predetermined time intervals and filtered through a membrane filter (0.45 μm). The CLX concentration was measured in the aqueous phase using high-performance liquid chromatography (HPLC) (Agilent Technologies Co., Ltd., USA), which was equipped with a ultraviolet C (UV-C) detector at 262 nm [36]. A reversed-phase C18 column (100 mm \times 4.6 mm) was also used as the HPLC column at a temperature of 25°C. The mobile phase contained acetonitrile and deionized water: 1:10 (V/V), along with ammonium acetate (1 molar) as a buffer at a flow rate of 1 ml/min. At each interval time, 20 μl of the solution was injected into the column and then measured at a fixed wavelength of 262 nm. The removal efficiency (%) of CLX was calculated via Eq. (6):

$$\text{Removal}(\%) = \frac{(C_0 - C_t)}{C_0} \times 100 \quad (6)$$

where C_0 and C_t are the initial concentration of CLX at the time (0) and concentration of CLX at the time (t), respectively.

Chemical oxygen demand (COD) was determined according to the standard methods for the examination of water and wastewater [37]. In addition, the total organic carbon (TOC) contents of CLX antibiotic was analyzed in a TOC analyzer (Elementar, Germany).

Liquid chromatography/mass spectrometry (LC/MS) (LC/MS-2010 A, Shimadzu, Japan) was applied to determine the degradation products of CLX. Scanning electron microscopy (SEM; FEINova NanoSEM45, USA) was performed to determine the particle size distribution of the catalyst. Additionally, energy-dispersive X-ray microanalysis (EDX; Bruker XFlash 6110, Germany) was performed to identify the constituents of the catalyst. Finally, X-ray diffraction (XRD) was carried out using a PANalytical diffractometer (USA) (Ultima IV).

3. Results and discussion

3.1. Morphological of catalyst

Fig. 2a indicates the SEM photograph of NiO nanoparticle and showing the morphology of the surface NiO, where

Table 1
Factors and levels in L_{16} orthogonal array and obtained results

Factors		Levels			
pH	–	3	5	7	9
CLX	Concentration (mg/L)	20	40	60	80
Hydrogen peroxide	Concentration (ml/L)	5	10	15	20
NiO	Dose (mg/L)	0.5	1	1.5	2
Time	Min.	15	30	45	60

No.	Factors					CRE ₁ ^a	CRE ₂	S/N
	pH	Hydrogen peroxide (ml/L)	NiO (mg/L)	CLX (mg/L)	Time (min)			
1	3	5	0.5	20	15	87	86.3	38.75
2	3	10	1	40	30	95.4	96	39.62
3	3	15	1.5	60	45	99.27	99.3	39.93
4	3	20	2	80	60	86.2	86.5	38.73
5	5	10	0.5	80	45	84	84.2	38.5
6	5	5	1	60	60	83.5	83.5	38.43
7	5	20	1.5	40	15	90.5	90	39.11
8	5	15	2	20	30	86.2	86.2	38.71
9	7	15	0.5	40	60	80	81.2	38.13
10	7	20	1	20	45	82.5	82	38.3
11	7	5	1.5	80	30	78.5	78.6	37.9
12	7	10	2	60	15	82.3	83	38.3
13	9	20	0.5	60	30	75.4	76	37.6
14	9	15	1	80	15	73.1	73.3	37.3
15	9	10	1.5	20	60	80	79.3	39.05
16	9	5	2	40	45	74	74.2	37.4

^a Constant-rate-of-extension

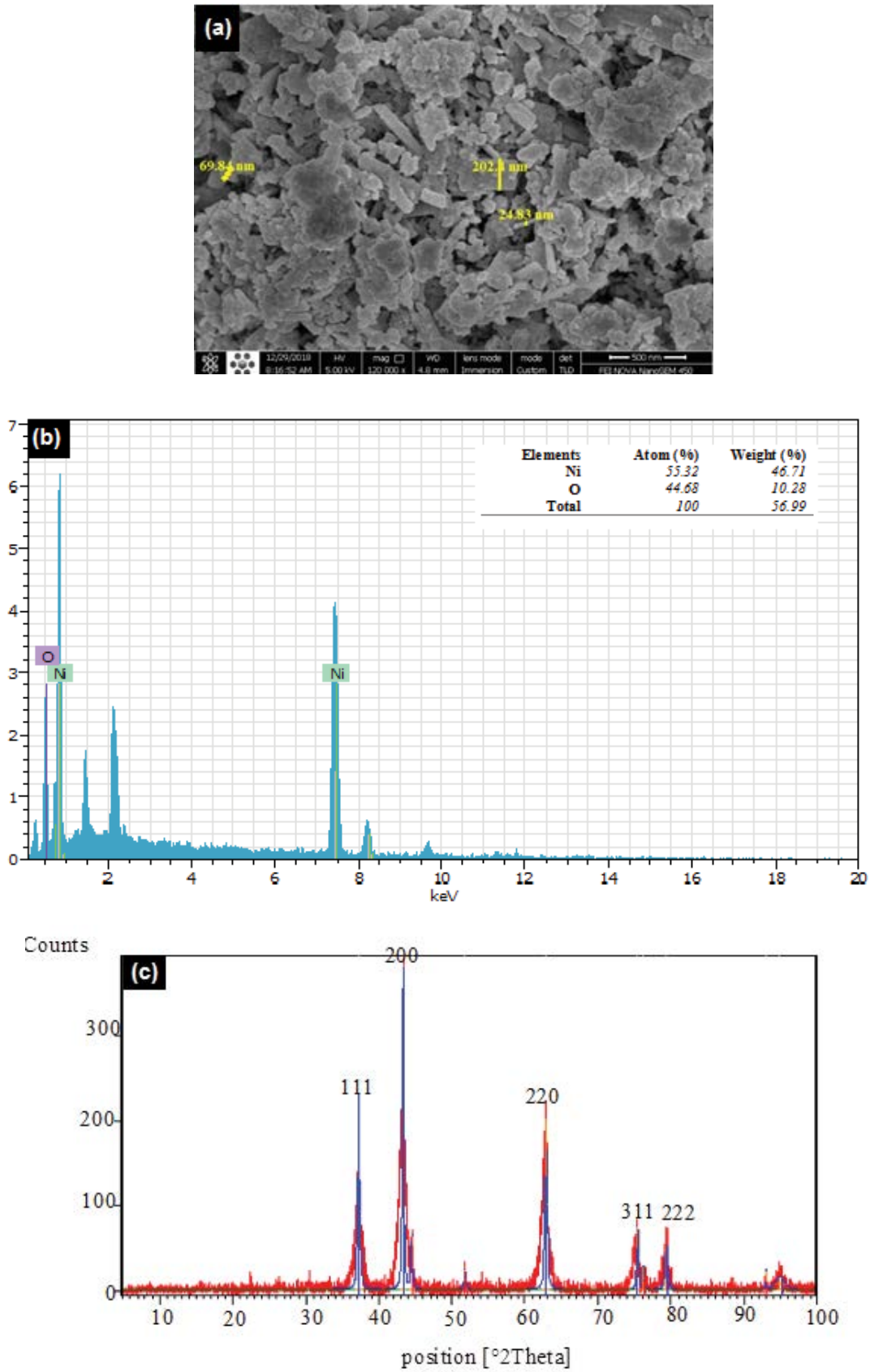


Fig. 2. (a) SEM image, (b) EDX image, and (c) XRD pattern of the NiO nanoparticles.

the smooth and uniform structures can be seen over the surface. Based on Fig. 2a, the NiO nanoparticle has an average diameter of 24.8–202 nm and was a tubular shape with heterogeneous pores. The attendance of well-distributed nonporous along the entire NiO can mostly raise the electrode/electrolyte contact area and is anticipated to be conducive to the ion transport. Fig. 2b presents the EDX photograph of NiO, which confirms that the achieved NiO certainly consists of Ni and O with a percentage of atom and weight as shown in the. Fig. 2b indicates the sharp peak, corresponding to Ni and O elements in the EDX analysis. The peaks revealed high purity of NiO nanoparticles, consisting of 81.5% nickel and 18% oxygen. According to the XRD pattern of NiO in Fig. 2c, different peaks located at 111, 200, 220, 311, and 222 crystal planes were obviously consisted of with NiO. No impurities were detected which proposes the high purity of monophasic NiO nanoparticles.

3.2. Effects of different parameters on CLX degradation

3.2.1. Effect of pH

The initial pH of the solution had a considerable effect on the degradation of pollutants using AOPs processes [25,28]. In chemical oxidation reactions, the pH of the solution influences the oxidation efficiency by affecting the generation of hydroxyl radicals [29]. To study the effects of initial pH on CLX degradation via the UV/hydrogen peroxide/NiO process, the experiments were carried out at different initial pH values from 3 to 9. The obtained CLX degradation rate in these pH ranges based on S/N ratio and mean values, which is presented in Fig. 3. It was found that the rate of CLX degradation was strongly pH-dependent. The degradation rates in acidic solutions are higher and decreased when the initial pH increased from 3 to 9. Therefore, the optimal CLX removal rate was obtained in acidic pH. It could be relevant to the role of hydroxyl radical, which is generated more abundantly under the acidic conditions to react with CLX through an electron-transferring mechanism. In addition, most of the CLX is separated into an ionic form ($pK_a = 6.88$) in acidic conditions, which has the greatest reactivity compared to unseparated CLX [38]. According to the results, when the initial pH was increased, the CLX degrading rate gradually decreased as

well. On the other hand, changes in the solution pH may result in changes in the hydrophobic property of CLX, in which less hydrophobic property occurred in acidic solution. Moreover, in the basic solution, the solubility and hydrophilicity of CLX were intensified, and therefore, the degradation rate was decreased. Furthermore, the pH_{zpc} of CLX was 2.29. These results are in agreement with the study by Azarpira et al. [39] regarding the removal of triclosan via UV/iodide/ZnO process. However, Massoudinejad et al. [40] reported enhanced degradation of arsenic under the UV/ H_2O_2 in the presence of ZnO nanoparticles. Also, Ebrahimi et al. [41] reported similar results for dye removal.

3.2.2. Effect of hydrogen peroxide concentration

Fig. 4 represents the effect of different initial hydrogen peroxide concentration (5–20 ml/L) on CLX degradation, based on S/N ratio and mean values. According to Fig. 4, CLX removal rate first improved by increasing the concentration of hydrogen peroxide from 5 to 10 ml/L. These results show that hydrogen peroxide plays a necessary role in CLX degradation. The improvement of CLX degradation by adding hydrogen peroxide is associated with hydroxyl radical ($E_0 = 2.8$ V in acidic pH) as an oxidizing agent according to Eq. (7) [6,42,43].



However, an increase in hydrogen peroxide concentration up to 10 ml/L led to a major adverse effect on CLX degradation. On the other hand, by increasing the initial hydrogen peroxide concentration, the scavenging activity increased to capture active radicals according to Eq. (8) [44].



Compared to hydroxyl radicals, the produced radicals (HO_2^\bullet) show much lower oxidation potential. In addition, hydrogen peroxide is decomposed to form water and oxygen if a large amount of hydrogen peroxide is used according to Eq. (9) [6].

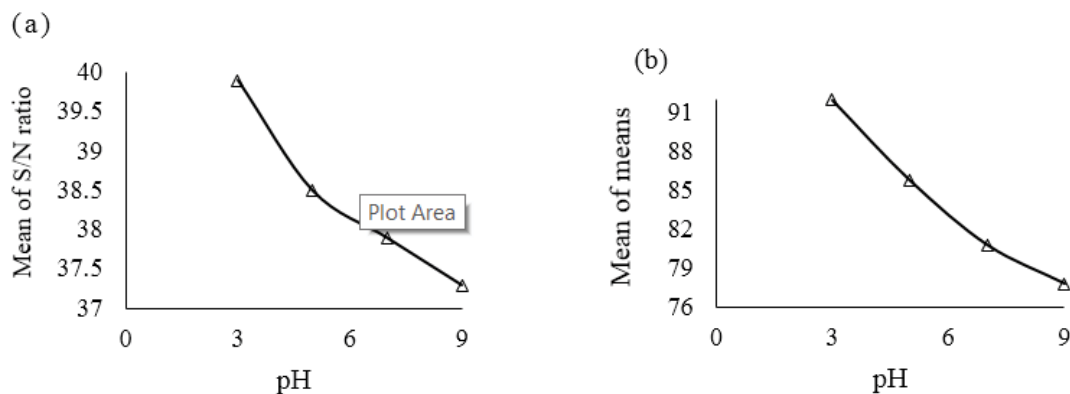


Fig. 3. Effect of pH on CLX degradation based on (a) S/N and (b) mean.

In this regard, Elmolla and Chaudhuri [25] studied the degradation of amoxicillin, cloxacillin, and ampicillin by hydrogen peroxide in the presence of UV-C irradiation and reported that higher degradation is highly dependent on the oxidant concentration.

3.2.3. Effect of CLX initial concentration

For evaluating the effect of initial CLX concentration on CLX degradation rate, experiments were designed using four levels of CLX ranging from 20 to 80 mg/L. The results are presented in Fig. 5. Based on the S/N ratio and mean values, CLX removal efficiencies decreased with increasing the CLX initial concentration from 20 to 80 mg/L. As shown, a lower CLX removal efficiency was obtained by increasing the initial CLX concentration at 80 mg/L. At low concentrations of CLX, hydroxyl radicals can comfortably eliminate a great percentage of CLX in the reaction reactor. However, by increasing the concentration of CLX, the number of hydroxyl radicals produced is not adequate for the complete degrading of CLX [45].

3.2.4. Effect of NiO dosages

The effect of the initial NiO dosage as catalyst ranging from 0.5 to 2 mg/L on the CLX degradation rate was

studied. The S/N ratio and mean values are illustrated in Fig. 6. Based on results, by increasing the catalyst concentration from 0.5 to 1.5 mg/L, the efficiency of CLX removal improved. This is due to the fact that the production of free hydroxyl radicals enhances by increasing the NiO dosage, which improved the CLX removal rate. However, adding an excessive dosage of NiO higher than the optimum level may reduce the removal efficiency of CLX. This may be related to the generation of Ni^{2+} , which scavenges the hydroxyl radicals, leading to a reduction in the CLX removal rate. Therefore, the NiO concentration of 1.5 mg/L was chosen for further experiments. Furthermore, several studies have reported that the photoabsorption of catalysts and the number of active sites strongly affect the degradation of pollutants. A suitable dosage of catalyst can improve the formation of electron/hole pairs, and lead to the generation of hydroxyl radicals for enhancing photocatalytic process [3,46]. On the other hand, the rise in the degradation efficiency may be related to the fact that the increase in the NiO nanoparticle concentration may lead to an improvement in the adsorbent surface of CLX. This is reliable for a particular value of nanoparticle concentration and, after this value, the degradation efficiency is decreased by increasing the nanoparticle concentration; it can be due to a decrease in the effective surface area which is consistent to the results of the study conducted by Panji et al. [47].

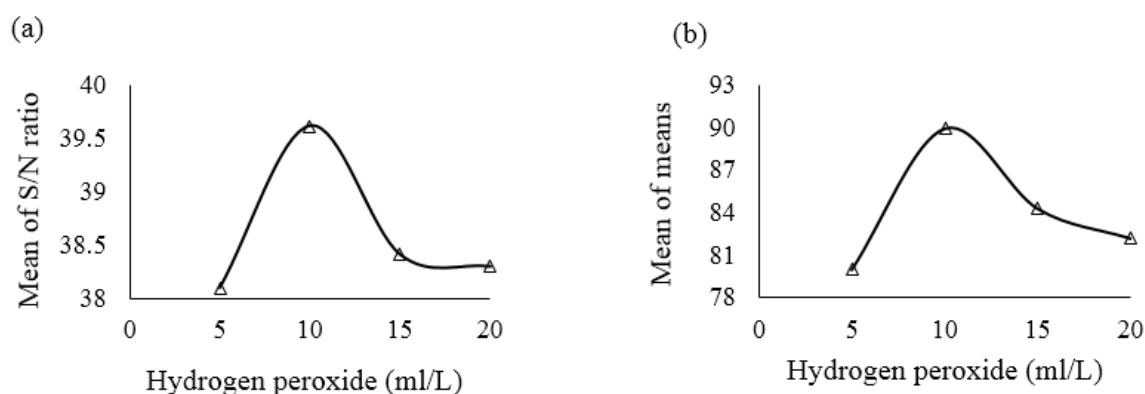


Fig. 4. Effect of hydrogen peroxide on CLX degradation based on (a) S/N and (b) mean.

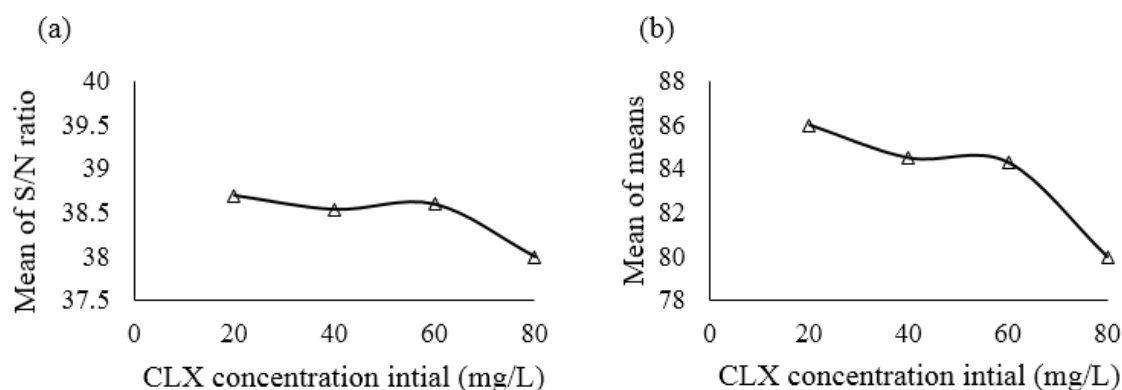


Fig. 5. Effect of initial CLX concentration based on (a) S/N and (b) mean.

3.2.5. Effect of contact time

To determine the effect of contact time on CLX removal efficiency, the experiments were conducted at different contact times in the range from 15 to 60 min. The results were based on S/N ratios and mean values, are indicated in Fig. 7. As shown, by increasing the reaction time, the removal efficiency is promoted and reaches a constant level at equilibrium state. The obtained results showed that increasing the reaction time also had direct effects on the removal efficiency, which is consistent with the results of studies conducted by Mizukoshi [15] and Zarei et al. [48].

3.3. CLX degrading by different systems

Fig. 8 compares CLX degrading in a different system, including NiO, hydrogen peroxide, UV, NiO/UV, hydrogen peroxide/UV, NiO/hydrogen peroxide, and NiO/hydrogen peroxide/UV. The experimental conditions were the following: UV irradiation, CLX = 20 mg/L, pH 3 and 60 min contact time. The result evidently illustrated that 1.5 mg/L NiO could achieve a 5% CLX removal rate, which is attributed to the limited oxidizing ability of NiO. As can be seen, the efficiency of CLX removal by the NiO/UV and hydrogen peroxide/UV systems are higher than single NiO, hydrogen peroxide, and UV systems. After 60 min, the removal of CLX was about 65% and 84% for the combined NiO/UV and hydrogen peroxide/UV respectively.

Also based on Fig. 8 the NiO/hydrogen peroxide had a catalytic efficiency 2.7 times that of hydrogen peroxide alone. This, in turn, shows that hydrogen peroxide has a lower oxidation rate [49]. The related results showed that CLX removal was refractory to the NiO induced oxygen activation, and the formation of hydroxyl radicals induced by the activation of NiO by UV irradiation which was not enough to continue the removal of CLX. According, the result showed that UV irradiation could be activated NiO via Eq. (10).



Due to the ability to generate OH^{\bullet} in the solution, UV irradiation could improve the photocatalytic AOPs efficiency [38]. As a result, following the addition of hydrogen peroxide as catalyst support to the solution with NiO and in the presence of the UV irradiation the CLX removal rate was enhanced and reached up to 95%. This phenomenon indicated that, in the presence of UV, a specific and synergistic effect exists between NiO and hydrogen peroxide. The synergistic effect may be defined by UV initiating which increased the mass transfer rate of the system.

3.4. Mineralization

Besides the degradation of recalcitrant pollutants, adequate mineralization in pollutants will lead to their

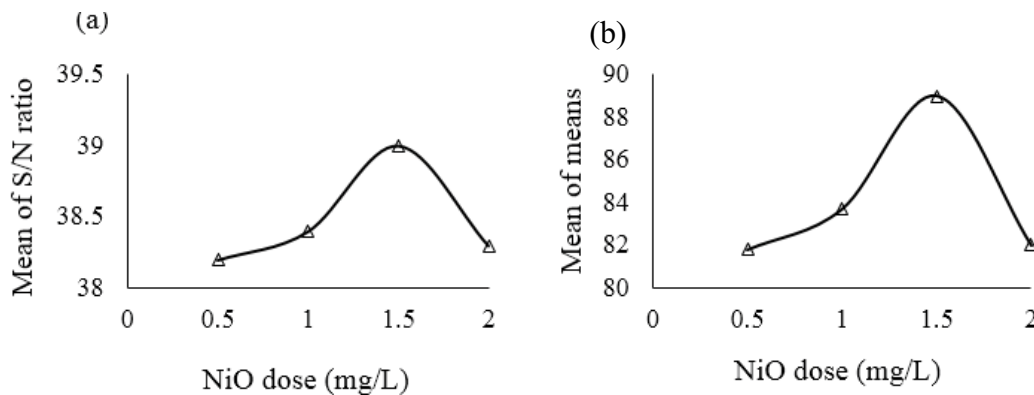


Fig. 6. Effect of initial NiO dosage based on (a) S/N and (b) mean.

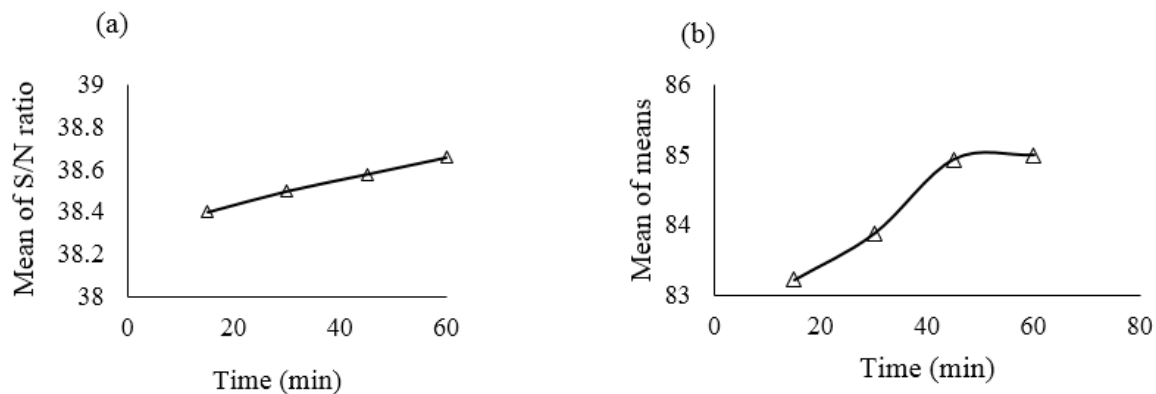


Fig. 7. Effect of contact time based on (a) S/N and (b) mean.

conversion into the water, carbon dioxide, or other mineral ions. This process can be an applicable alternative for the treatment of contaminated wastewater with organic pollutants [50]. It has been suggested that the amount of organic pollutants is higher than the extent of mineralization [51]. For evaluating CLX mineralization, COD and TOC were measured during the CLX degradation process at an initial CLX concentration of 20 mg/L. The experimental conditions were conducted based on the obtained optimal parameters, including pH of solution 3, NiO dosage of 1.5 mg/L, and hydrogen peroxide concentration of 10 ml/L at different contact times. The results are shown in Fig. 9. As shown the rates of CLX mineralization for COD and TOC removal were 83% and 68% within 60 min contact time, respectively. Under the same operational conditions, the results indicated that the CLX degradation rate was 98%, which is much higher than the removal rates of COD and TOC. This could be due to the fact that CLX was transformed into intermediate metabolites. This finding is in accordance with a report by Rizzo et al. on the degradation of diclofenac using photocatalyst oxidation [52]. They reported that the COD removal rate was 85%, whereas its degradation rate was 94%.

3.5. Optimization of experimental and ANOVA analysis

In the present study, five controllable factors, that is, pH of solution, NiO dosage, hydrogen peroxide concentration, initial CLX concentration, and contact time, were selected as input variables. These factors were removed at four levels based on the L_{16} OA method, as shown in Table 1. The CLX removal percentage was evaluated as four responses in the binary mixture, using the Taguchi L_{16} array method. Also, the experimental data were converted to the S/N ratio according to Eq. 9 [53]. Table 1 presents the response tables for S/N ratios. S/N ratio represents the optimal database with respect to the minimum deviation [54] and helps determine the optimum values for each factor [55]. The optimum experimental conditions include the pH (Level 1 (3)), NiO (Level 3 (1.5 mg/L)), hydrogen peroxide (Level 2 (10 ml/L)), CLX initial concentration (Level 1 (20 mg/L)). The results indicated that the optimum experimental conditions, the mean effect and S/N ratio measurements were similar for optimal conditions. Moreover, to determine the most effective parameter for degradation of CLX with the UV/hydrogen peroxide/NiO process, ANOVA was performed. The ANOVA results regarding CLX removal are presented in Table 2. The degree of freedom

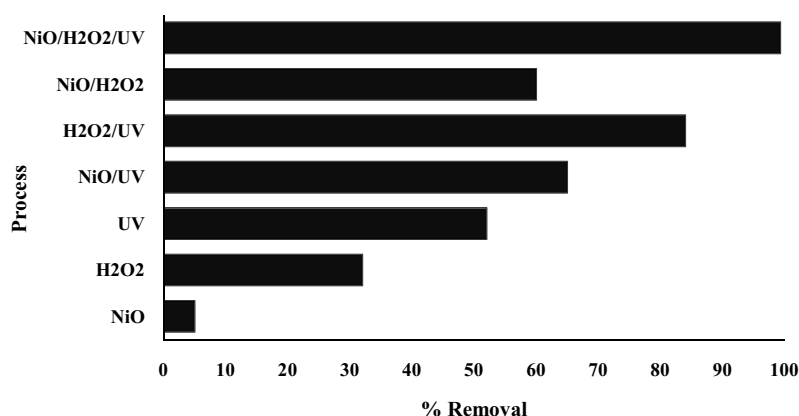


Fig. 8. Effect of different systems on CLX degradation.

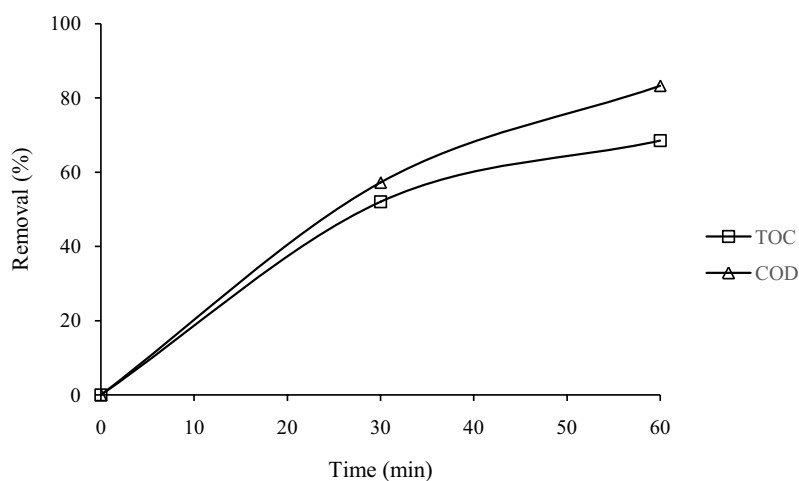


Fig. 9. COD and TOC Removal rate in optimum conditions.

Table 2
ANOVA results for CLX degradation

Factor	DOF ^a	S ^b	V ^c	F ^d	P ^e
pH	3	442.540	147.513	49.54	56.2
NiO	3	148.388	49.436	16.61	18.84
Hydrogen peroxide	3	110.183	36.728	12.33	13.99
CLX initial concentration	3	77.344	25.781	8.66	9.82
Residual error	3	8.933	9.978	–	1.13
Total	15	787.388	–	–	100

^aDegrees of freedom

^bSum of squares

^cVariance

^dF-ratio

^ePercentage contribution

(DOF) was three for each factor, and the total DOF was 15. This indicates the influence participation of each factor on degradation. The results of ANOVA revealed that the most significant factor for CLX degradation was pH (56.2 %), and the lowest factor was time contact (1.13%). Furthermore, optimal conditions for degradation of CLX, including pH, NiO dosage, hydrogen peroxide concentration and initial CLX concentration, were determined based on S/N ratios at Level 1, Level 3, Level 2, and Level 1, respectively (Table 3). The optimal conditions were as follows: pH, 3; NiO dosage, 1.5 mg/L; hydrogen peroxide concentration 10 ml/L; CLX initial concentration, 20 mg/L; and contact time, 60 min.

3.6. CLX degradation pathway

According to the literature, oxygen and hydroxyl radicals are dominated in the AOPs processes based on hydrogen peroxide degrading organic material [56,57]. To study the degradation pathway of CLX with the UV/hydrogen peroxide/NiO process, the LC/MS technique was used to detect the intermediates. Intermediates detection was conducted by comparing molecular structure spectra with CLX degradation intermediates found in other AOPs [58], which are represented in Table 3. According to the referred mechanism and the molecular structures of identified intermediates, the transformation pathway and mechanism for degradation of CLX could be proposed as shown in scheme 1. Other studies clearly indicated that the oxygen radical reacts with antibiotics via three mechanisms including, hydroxylation, oxidation, and electron transfer [59]. The pathway (A) (Fig. 10), is related to attacking hydroxyl and oxygen radicals to the CLX molecules to generate 4-(hydroxymethyl) phenyl)sulfonyl-dimethyl-phenylazanium and 4-(4-ethyl-3,5-dimethyl-1,3-thiazol-3-ium-2-yl)-N,N-dimethylaniline which could be further degraded to 1-(3,5-dimethyladamantan-1-yl)-2-(1,3-thiazol-5-yl)ethan-1-amine, phenethylammonium and butylcarbamoyl through hydroxylation mechanism. In addition, these intermediate compounds can induce hydroxylation to generate diethylpropylamine and isohexylamine leading to the formation of CO₂, H₂O, and inorganic ions. The pathway (B), involves attacking oxygen radicals to CLX antibiotic and generate butyl 5-(1,4λ²-diazinan-1-yl) pentanoate via oxidation mechanism. Also, oxygen radicals can selectively react with this organic

compound and generate diethylpropylamine and isohexylamine via the same mechanism. In pathway (C), an electron transfer mechanism was suggested in which CLX molecules could be changed to 2-tert-butyl-1-(2,5-diethoxyphenyl) guanidine and then 1-[3-(1-aminoethyl) phenyl]-3-pentylurea. This aromatic hydrocarbon would be degraded to generate 1-oxido-3-pyrimidine which would be further degraded to CO₂ and H₂O.

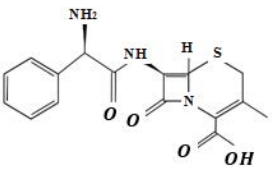
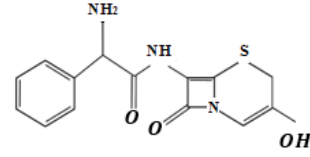
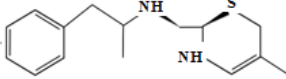
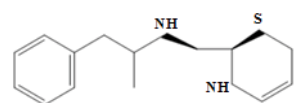
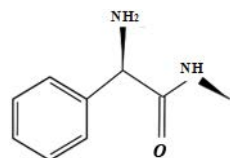
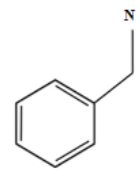
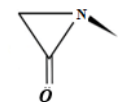
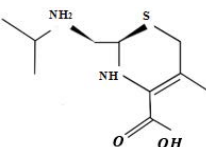
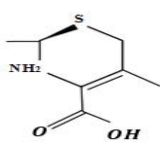
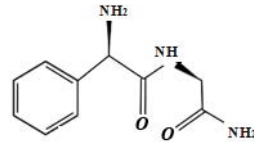
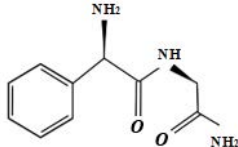
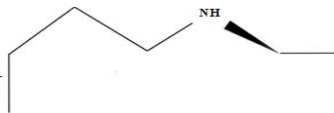
3.7. Kinetic analysis

Chemical kinetics is appropriate to evaluate the rate of chemical compounds reactions. The rate of a reaction could be described by decreasing the concentration of a reactant in reaction time or raised the concentration of their intermediate product per reaction time [45]. In this study, the pseudo-first-order, and the pseudo-second-order models were applied for CLX degrading and were calculated using Eqs. (11) and (12). In this study, the kinetics of the CLX antibiotic degrading was investigated in optimum conditions using first, and second-order kinetics models. The results were presented in Fig. 11 and Table 4. According to the results, the regression coefficients (R²) of the kinetic model for the first-order and the second-order were estimated as 0.97 and 0.85, respectively. Based on the results, the pseudo-first-order model was obtained with a considerable coefficient of correlation (R²), which was the preferable model to fit the data of CLX removal compared to other kinetics models. The experimental result showed that the hydrogen peroxide/NiO composite was an efficient degraded composite for the CLX degradation from aqueous solution. The rate constant (k) obtained for CLX antibiotic degradation using the NiO/hydrogen peroxide/UV hybrid process was 0.0255 min⁻¹. These results are according to the results of the studies conducted by Seid-Mohammadi et al. [45], Rocha et al. [60], and Samarghandi et al. [61].

$$\ln\left(\frac{C_0}{C_t}\right) = -k_1 t \quad (11)$$

$$\frac{1}{C_t} - \frac{1}{C_0} = -K_1 t \quad (12)$$

Table 3
Intermediate compounds of CLX degradation using UV/hydrogen peroxide/NiO

No.	Molecular structure	Formula	International Union of Pure and Applied Chemistry name	Molar mass
1		$C_{16}H_{17}N_3O_4S$	Cephalexin	347.1
2		$C_{15}H_{18}NO_3S$	4-(hydroxymethyl)phenyl[sulfonyl-dimethyl-phenyl]phenylazanium	306
3		$C_{15}H_{21}N_2S$	4-(4-ethyl-3,5-dimethyl-1,3-thiazol-3-ium-2-yl)-N,N-dimethylaniline	261
4		$C_{17}H_{26}N_2S$	1-(3,5-dimethyladamantan-1-yl)-2-(1,3-thiazol-5-yl)ethan-1-amine	290
5		$C_{12}H_{19}N_2O$	1-oxido-3-(4-pyrrolidin-1-ylbut-2-ynyl) pyrimidine	207
6		$C_8H_{12}N$	Phenethylammonium	122
7		C_5H_8NO	Butylcarbamoyl	98
8		$C_{13}H_{25}N_2O_2S$	Butyl 5-(1,4lambda2-diazinan-1-yl) pentanoate	273
9		$C_{10}H_{18}NO_2S$	1lambda2-Azinan-4-yl pentanoate	216
10		$C_{15}H_{25}N_3O_2$	2-tert-butyl-1-(2,5-diethoxyphenyl)guanidine	279
11		$C_{14}H_{23}N_3O$	1-[3-(1-aminoethyl)phenyl]-3-pentylurea	249
12		$C_6H_{15}N$	Isohexylamine	101
13		$C_5H_{13}N$	Diethylpropylamine	87

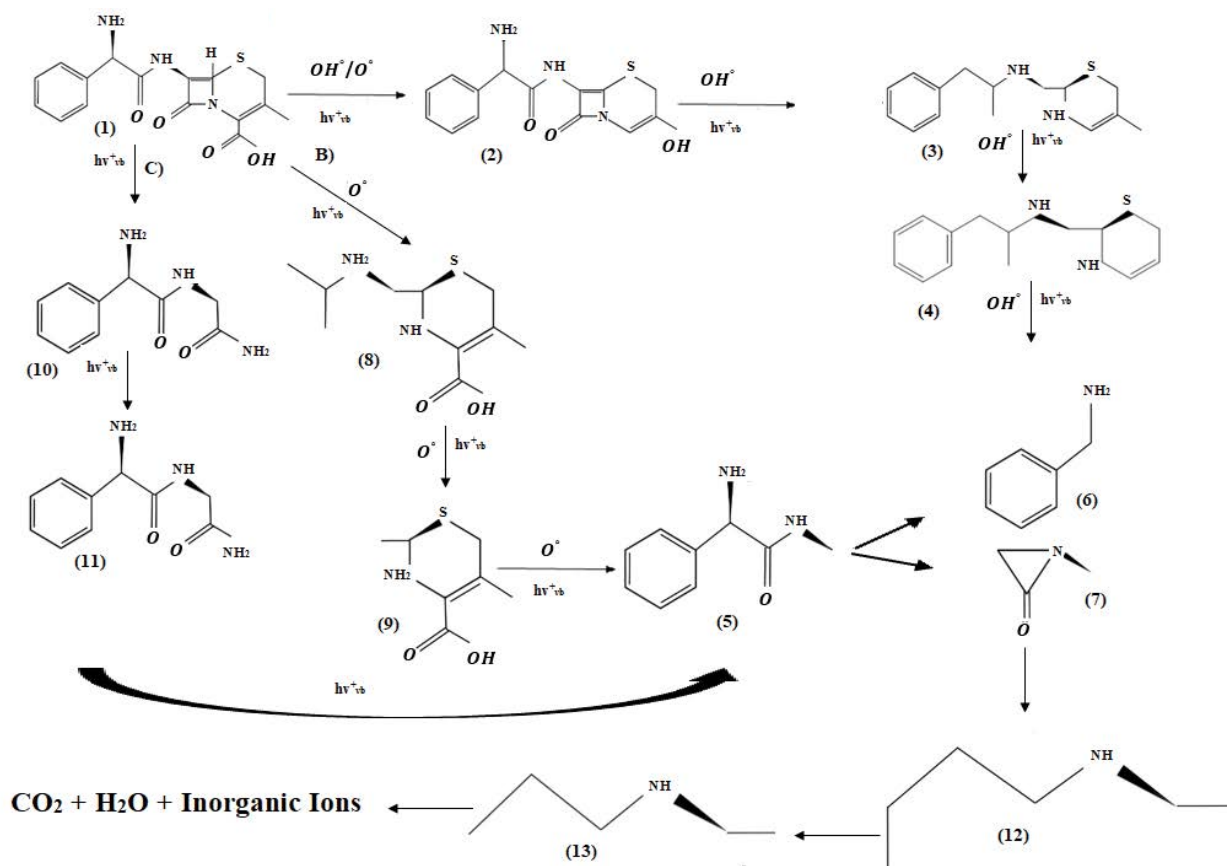


Fig. 10. Proposed degradation pathway of CLX degradation using the UV/hydrogen peroxide/NiO process.

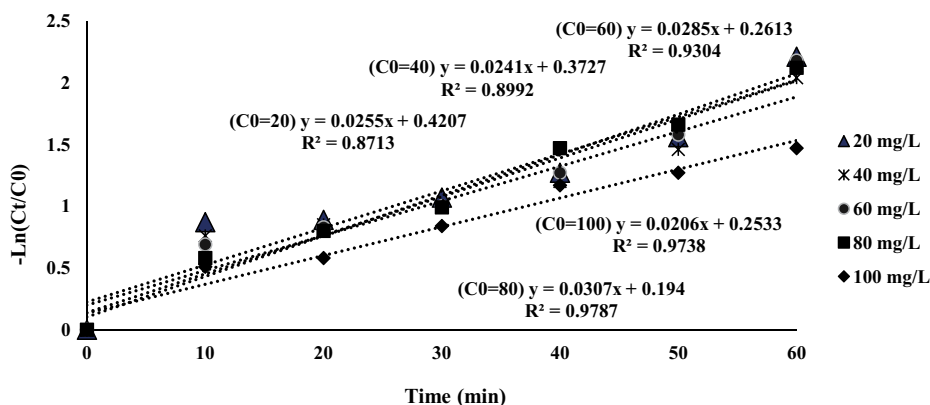


Fig. 11. The pseudo-first-order plot for removing CLX utilizes the UV/NiO/hydrogen peroxide system.

where C_0 and C_t are the initial and final concentrations of CLX antibiotics, respectively, and K is a constant of removal value; K value is equal to the slope of the plot of $\ln(C_0/C_t)$ vs. time t . Also, Table 5 shows a comparison between other photocatalyst studies with the current study.

4. Conclusion

In the present study, Taguchi's OA experimental design was used to determine the optimal operational parameters

including pH of solution, NiO dosage, hydrogen peroxide concentration, contact time, and CLX initial concentration degrading CLX from aqueous solution using UV/hydrogen peroxide/NiO system. The effect of each parameter was evaluated using ANOVA. According to ANOVA results, the pH of the solution and CLX initial concentration had the highest and lowest effect on CLX degradation, respectively. The CLX removal rate decreased with an increase in pH value from 3 to 11. Increased NiO nanoparticle and hydrogen peroxide resulted in an enhanced CLX degradation

Table 4
Kinetic parameters of CLX removal by the NiO/hydrogen peroxide/UV AOPs

C_0 (mg/L)	Pseudo-first-order		Second-order	
	K (min^{-1})	R^2	K (L/mg min)	R^2
$C_0 = 20$ mg/L	0.03	0.87	0.006	0.75
$C_0 = 40$ mg/L	0.02	0.90	0.002	0.74
$C_0 = 60$ mg/L	0.03	0.93	0.002	0.78
$C_0 = 80$ mg/L	0.03	0.98	0.001	0.92

Table 5
Comparison of antibiotic removal results of the present study by the photocatalytic process with other studies

Reference	Year	Antibiotic	Process	Reaction kinetic	Efficiency removal (%)
Michael et al. [62]	2020	Ciprofloxacin, sulfamethoxazole	UV-C/ H_2O_2 and sunlight/ H_2O_2	First-order	99
Liu et al. [63]	2020	Ofloxacin, levofloxacin	UV/ H_2O_2 and UV/persulfate	First-order	96
Pan et al. [64]	2019	Oxytetracycline, tetracycline, sulfadiazine	UV/pre-magnetized $\text{Fe}^0/\text{H}_2\text{O}_2$	First-order	97.2
Godini et al. [65]	2019	Impanel/cilastatin	UV-C/ $\text{Fe}^{2+}/\text{H}_2\text{O}_2$	First-order	100
Jiang et al. [66]	2019	Cefotaxime	UV + ferrihydrite/ $\text{TiO}_2 + \text{H}_2\text{O}_2$	First-order	99.3
Seid-Mohammadi et al. [36]	2019	Cephalexin	MgO/granular activated carbon/UV	First-order	98
Zhang et al. [67]	2016	Sulfonamide	UV/ H_2O_2	First-order	99
This study	2020	CLX	NiO/ H_2O_2 /UV	First-order	99.2

rate. The optimum condition for degradation of CLX were pH = 3, NiO = 1.5 mg/L, hydrogen peroxide = 10 ml/L, CLX initial concentration = 20 mg/L, and contact time = 60 min. In the case of mineralization, COD and TOC removal rates were 83% and 68% achieved in optimum conditions after 60 min irradiation time, respectively. Based on identified intermediates, various products were recognized during the CLX degradation process and based on LC/MS analysis and literature three degradation pathways were proposed. This study indicates the activation of hydrogen peroxide by NiO in the presence of UV irradiation as an effective method for treating wastewater containing CLX.

Acknowledgment

This research was financially supported by the Hamadan University of Medical Sciences (Grant No. 9612228291).

References

- [1] G. Nazari, H. Abolghasemi, M. Esmaili, Batch adsorption of cephalexin antibiotic from aqueous solution by walnut shell-based activated carbon, *J. Taiwan Inst. Chem. Eng.*, 58 (2016) 357–365.
- [2] A. Gulkowska, H.W. Leung, M.K. So, S. Taniyasu, N. Yamashita, L.W.Y. Yeung, B.J. Richardson, A.P. Lei, J.P. Giesy, P.K.S. Lam, Removal of antibiotics from wastewater by sewage treatment facilities in Hong Kong and Shenzhen, China, *Water Res.*, 42 (2008) 395–403.
- [3] Q.Q. Zhang, A. Jia, Y. Wan, H. Liu, K.P. Wang, H. Peng, Z.M. Dong, J.Y. Hu, Occurrences of three classes of antibiotics in a natural river basin: association with antibiotic-resistant *Escherichia coli*, *Environ. Sci. Technol.*, 48 (2014) 14317–14325.
- [4] I. Michael, L. Rizzo, C.S. McArdeell, C.M. Manaia, C. Merlin, T. Schwartz, C. Dagot, D. Fatta-Kassinos, Urban wastewater treatment plants as hotspots for the release of antibiotics in the environment: a review, *Water Res.*, 47 (2013) 957–995.
- [5] L. Rizzo, C. Manaia, C. Merlin, T. Schwartz, C. Dagot, M.C. Ploy, I. Michael, D. Fatta-Kassinos, Urban wastewater treatment plants as hotspots for antibiotic resistant bacteria and genes spread into the environment: a review, *Sci. Total Environ.*, 447 (2013) 345–360.
- [6] A. Seidmohammadi, R. Amiri, J. Faradmal, M. Lili, G. Asgari, UVA-LED assisted persulfate/nZVI and hydrogen peroxide/nZVI for degrading 4-chlorophenol in aqueous solutions, *Korean J. Chem. Eng.*, 35 (2018) 694–701.
- [7] N.H. Tran, H.J. Chen, M. Reinhard, F.J. Mao, K.Y.-H. Gin, Occurrence and removal of multiple classes of antibiotics and antimicrobial agents in biological wastewater treatment processes, *Water Res.*, 104 (2016) 461–472.
- [8] F. Lüddecke, S. Heß, C. Gallert, J. Winter, H. Güde, H. Löffler, Removal of total and antibiotic resistant bacteria in advanced wastewater treatment by ozonation in combination with different filtering techniques, *Water Res.*, 69 (2015) 243–251.
- [9] B. Kamarehie, J. Mohamadian, S.A. Mousavi, G. Asgari, Y.D. Shahamat, Aniline degradation from aqueous solution using electro/ Fe^{2+} /peroxydisulphate process, *Desal. Water Treat.*, 80 (2017) 337–343.
- [10] M.M. Amin, F. Teimouri, M. Sadani, M.A. Karami, Application of enhanced nZnO photocatalytic process with ultrasonic wave in formaldehyde degradation from aqueous solution, *Desal. Water Treat.*, 57 (2016) 9455–9464.
- [11] Y.-H. Chuang, A. Szczuka, F. Shabani, J. Munoz, R. Aflaki, S.D. Hammond, W.A. Mitch, Pilot-scale comparison of microfiltration/reverse osmosis and ozone/biological activated carbon with UV/hydrogen peroxide or UV/free chlorine AOP treatment for controlling disinfection byproducts during wastewater reuse, *Water Res.*, 152 (2019) 215–225.
- [12] X.C. Liu, Y.Y. Zhou, J.C. Zhang, L. Luo, Y. Yang, H.L. Huang, H. Peng, L. Tang, Y. Mu, Insight into electro-Fenton and

- photo-Fenton for the degradation of antibiotics: mechanism study and research gaps, *Chem. Eng. J.*, 347 (2018) 379–397.
- [13] T.H. de Oliveira Norte, R.B.P. Marcelino, F.H.A. Medeiros, R.P.L. Moreira, C.C. Amorim, R.M. Lago, Ozone oxidation of β -lactam antibiotic molecules and toxicity decrease in aqueous solution and industrial wastewaters heavily contaminated, *Ozone Sci. Eng.*, 40 (2018) 385–391.
- [14] B. Kamarehie, A. Jafari, M. Ghaderpoori, M.A. Karami, K. Mousavi, A. Ghaderpoury, Catalytic ozonation process using PAC/ γ -Fe₂O₃ to Alizarin Red S degradation from aqueous solutions: a batch study, *Chem. Eng. Commun.*, 206 (2019) 898–908.
- [15] Y. Mizukoshi, Effects of sonication on photocatalytic reforming of aqueous glycerol solution, *Ultrason. Sonochem.*, 51 (2019) 182–185.
- [16] Q.Q. Liu, J.Y. Shen, X.F. Yang, T.R. Zhang, H. Tang, 3D reduced graphene oxide aerogel-mediated Z-scheme photocatalytic system for highly efficient solar-driven water oxidation and removal of antibiotics, *Appl. Catal., B*, 232 (2018) 562–573.
- [17] X.X. He, A.A. de la Cruz, D.D. Dionysiou, Destruction of cyanobacterial toxin cylindrospermopsin by hydroxyl radicals and sulfate radicals using UV-254 nm activation of hydrogen peroxide, persulfate and peroxymonosulfate, *J. Photochem. Photobiol., A*, 251 (2013) 160–166.
- [18] M. Ghaderpoori, M.H. Dehghani, Investigating the removal of linear alkyl benzene sulfonate from aqueous solution by ultraviolet irradiation and hydrogen peroxide process, *Desal. Water Treat.*, 57 (2016) 15208–15212.
- [19] L.V. de Souza Santos, A.M. Meireles, L.C. Lange, Degradation of antibiotics norfloxacin by Fenton, UV and UV/H₂O₂, *J. Environ. Manage.*, 154 (2015) 8–12.
- [20] R. Ebrahimi, M. Mohammadi, A. Maleki, A. Jafari, B. Shahmoradi, R. Rezaee, M. Safari, H. Daraei, O. Gaihi, K. Yetilmezsoy, S.H. Puttaiah, Photocatalytic degradation of 2,4-dichlorophenoxyacetic acid in aqueous solution using Mn-doped ZnO/graphene nanocomposite under LED radiation, *J. Inorg. Organomet. Polym. Mater.*, 30 (2020) 923–934.
- [21] Z. Cao, X. Liu, J. Xu, J. Zhang, Y. Yang, J.L. Zhou, X.H. Xu, G.V. Lowry, Removal of antibiotic florfenicol by sulfide-modified nanoscale zero-valent iron, *Environ. Sci. Technol.*, 51 (2017) 11269–11277.
- [22] Y.P. Ji, Z.C. Pan, D.H. Yuan, B. Lai, Advanced treatment of the antibiotic production wastewater by ozone/zero-valent iron process, *Clean-Soil Air Water*, 46 (2018) 1700666.
- [23] F. Kord Mostafapour, E. Bazrafshan, D. Belark, N. Khoshnamvand, Survey of photo-catalytic degradation of ciprofloxacin antibiotic using copper oxide nanoparticles (UV/CuO) in aqueous environment, *J. Rafsanjan Univ. Med. Sci.*, 15 (2016) 307–318.
- [24] C. Bojer, J. Schöbel, T. Martin, M. Ertl, H. Schmalz, J. Breu, Clinical wastewater treatment: photochemical removal of an anionic antibiotic (ciprofloxacin) by mesostructured high aspect ratio ZnO nanotubes, *Appl. Catal., B*, 204 (2017) 561–565.
- [25] E.S. Elmolla, M. Chaudhuri, Photocatalytic degradation of amoxicillin, ampicillin and cloxacillin antibiotics in aqueous solution using UV/TiO₂ and UV/H₂O₂/TiO₂ photocatalysis, *Desalination*, 252 (2010) 46–52.
- [26] F. Asadi, A. Dargahi, A. Almasi, E. Moghobe, Red Reactive 2 dye removal from aqueous solutions by pumice as a low-cost and available adsorbent, *Arch. Hyg. Sci.*, 5 (2016) 145–152.
- [27] Z.Q. Fang, X.Q. Qiu, J.H. Chen, X.H. Qiu, Degradation of metronidazole by nanoscale zero-valent metal prepared from steel pickling waste liquor, *Appl. Catal., B*, 100 (2010) 221–228.
- [28] A. Zuurro, M. Fidaleo, M. Fidaleo, R. Lavecchia, Degradation and antibiotic activity reduction of chloramphenicol in aqueous solution by UV/H₂O₂ process, *J. Environ. Manage.*, 133 (2014) 302–308.
- [29] Y. Deng, R.Z. Zhao, Advanced oxidation processes (AOPs) in wastewater treatment, *Curr. Pollut. Rep.*, 1 (2015) 167–176.
- [30] Y. Yang, Y. Cao, J. Jiang, X.L. Lu, J. Ma, S.Y. Pang, J. Li, Y.Z. Liu, Y. Zhou, C.T. Guan, Comparative study on degradation of propranolol and formation of oxidation products by UV/H₂O₂ and UV/persulfate (PDS), *Water Res.*, 149 (2019) 543–552.
- [31] M. Kaladhar, K.V. Subbaiah, C.S. Rao, K.N. Rao, Application of Taguchi approach and utility concept in solving the multi-objective problem when turning AISI 202 austenitic stainless steel, *J. Eng. Sci. Technol. Rev.*, 4 (2011) 1791–2377.
- [32] A. Fakhri, S. Behrouz, Comparison studies of adsorption properties of MgO nanoparticles and ZnO–MgO nanocomposites for linezolid antibiotic removal from aqueous solution using response surface methodology, *Process Saf. Environ.*, 94 (2015) 37–43.
- [33] T.T. Wu, J.D. Englehardt, A new method for removal of hydrogen peroxide interference in the analysis of chemical oxygen demand, *Environ. Sci. Technol.*, 46 (2012) 2291–2298.
- [34] J. Zolgharnein, M. Rastgordani, Optimization of simultaneous removal of binary mixture of indigo carmine and methyl orange dyes by cobalt hydroxide nano-particles through Taguchi method, *J. Mol. Liq.*, 262 (2018) 405–414.
- [35] M.R. Sohrabi, A. Khavaran, S. Shariati, S. Shariati, Removal of Carmoisine edible dye by Fenton and photo Fenton processes using Taguchi orthogonal array design, *Arabian J. Chem.*, 10 (2017) S3523–S3531.
- [36] H.T. Elbalkiny, A.M. Yehia, S.M. Riad, Y.S. Elsharty, Removal and tracing of cephalosporins in industrial wastewater by SPE-HPLC: optimization of adsorption kinetics on mesoporous silica nanoparticles, *J. Anal. Sci. Technol.*, 10 (2019) 2093–3371.
- [37] WEF, APHA, Standard Methods for the Examination of Water and Wastewater, American Public Health Association (APHA), Washington, DC, USA, 2005.
- [38] A. Seid-Mohammadi, M. Bahrami, S. Omari, F. Asadi, Removal of cephalixin from aqueous solutions using magnesium oxide/granular activated carbon hybrid photocatalytic process, *Avicenna J. Environ. Health Eng.*, 6 (2019) 51–59.
- [39] H. Azarpira, M. Sadani, M. Abtahi, N. Vaezi, S. Rezaei, Z. Atafar, S.M. Mohseni, M. Sarkhosh, M. Ghaderpoori, H. Keramati, R.H. Pouya, A. Akbari, V. Fanai, Photo-catalytic degradation of triclosan with UV/iodide/ZnO process: performance, kinetic, degradation pathway, energy consumption and toxicology, *J. Photochem. Photobiol., A*, 371 (2019) 423–432.
- [40] M. Massoudinejad, H. Keramati, M. Ghaderpoori, Investigation of photo-catalytic removal of arsenic from aqueous solutions using UV/H₂O₂ in the presence of ZnO nanoparticles, *Chem. Eng. Commun.*, (2019) 1–11.
- [41] R. Ebrahimi, K. Hossienzadeh, A. Maleki, R. Ghanbari, R. Rezaee, M. Safari, B. Shahmoradi, H. Daraei, A. Jafari, K. Yetilmezsoy, S.H. Puttaiah, Effects of doping zinc oxide nanoparticles with transition metals (Ag, Cu, Mn) on photocatalytic degradation of Direct Blue 15 dye under UV and visible light irradiation, *J. Environ. Health Sci.*, 17 (2019) 479–492.
- [42] A. Babuponnusami, K. Muthukumar, Advanced oxidation of phenol: a comparison between Fenton, electro-Fenton, sono-electro-Fenton and photo-electro-Fenton processes, *Chem. Eng. J.*, 183 (2012) 1–9.
- [43] H. Yang, L.Y. Mei, P.C. Wang, J. Genereux, Y.S. Wang, B. Yi, C.T. Au, L.M. Dang, P.Y. Feng, Photocatalytic degradation of norfloxacin on different TiO_{2-x} polymorphs under visible light in water, *RSC Adv.*, 7 (2017) 45721–45732.
- [44] G.Z. Kyzas, K.A. Matis, Nano-adsorbents for pollutants removal: a review, *J. Mol. Liq.*, 203 (2015) 159–168.
- [45] A. Seid-Mohammadi, G. Asgarai, Z. Ghorbanian, A. Dargahi, The removal of cephalixin antibiotic in aqueous solutions by ultrasonic waves/hydrogen peroxide/nickel oxide nanoparticles (US/H₂O₂/NiO) hybrid process, *Sep. Sci. Technol.*, 55 (2020) 1–11.
- [46] A.H. Mahvi, A. Maleki, R. Rezaee, M. Safari, Reduction of humic substances in water by application of ultrasound waves and ultraviolet irradiation, *Iran. J. Environ. Health*, 6 (2009) 233–240.
- [47] A. Panji, L.U. Simha, B.M. Nagabhushana, Heavy metals removal by nickel-oxide nanoparticles synthesised by lemon juice extract, *Int. J. Eng. Manage. Res.*, 6 (2016) 287–291.
- [48] M. Zarei, A.R. Khataee, R. Ordikhani-Seyedlar, M. Fathinia, Photoelectro-Fenton combined with photocatalytic process for degradation of an azo dye using supported TiO₂ nanoparticles

- and carbon nanotube cathode: neural network modeling, *Electrochim. Acta*, 55 (2010) 7259–7265.
- [49] G. Moussavi, A.A. Aghapour, K. Yaghmaei, The degradation and mineralization of catechol using ozonation catalyzed with MgO/GAC composite in a fluidized bed reactor, *Chem. Eng. J.*, 249 (2014) 302–310.
- [50] D. Shahidi, R. Roy, A. Azzouz, Advances in catalytic oxidation of organic pollutants – prospects for thorough mineralization by natural clay catalysts, *Appl. Catal., B*, 174 (2015) 277–292.
- [51] R. Kaplan, B. Erjavec, G. Dražić, J. Grdadolnik, A. Pintar, Simple synthesis of anatase/rutile/brookite TiO₂ nanocomposite with superior mineralization potential for photocatalytic degradation of water pollutants, *Appl. Catal., B*, 181 (2016) 465–474.
- [52] L. Rizzo, S. Meric, D. Kassinos, M. Guida, F. Russo, V. Belgiorno, Degradation of diclofenac by TiO₂ photocatalysis: UV absorbance kinetics and process evaluation through a set of toxicity bioassays, *Water Res.*, 43 (2009) 979–988.
- [53] M. Rahmani, M. Kaykhaii, M. Sasaki, Application of Taguchi L16 design method for comparative study of ability of 3A zeolite in removal of Rhodamine B and Malachite green from environmental water samples, *Spectrochim. Acta, Part A*, 188 (2018) 164–169.
- [54] M. Dehghani, S. Behzadi, M.S. Sekhavatjou, Optimizing Fenton process for the removal of amoxicillin from the aqueous phase using Taguchi method, *Desal. Water Treat.*, 57 (2016) 6604–6613.
- [55] S. Varala, A. Kumari, B. Dharanija, S.K. Bhargava, R. Parthasarathy, B. Satyavathi, Removal of thorium (IV) from aqueous solutions by deoiled karanja seed cake: optimization using Taguchi method, equilibrium, kinetic and thermodynamic studies, *J. Environ. Chem. Eng.*, 4 (2016) 405–417.
- [56] J.L. Wang, L.J. Xu, Advanced oxidation processes for wastewater treatment: formation of hydroxyl radical and application, *Crit. Rev. Env. Sci. Technol.*, 42 (2012) 251–325.
- [57] P. Fernández-Castro, M. Vallejo, M.F. San Román, I. Ortiz, Insight on the fundamentals of advanced oxidation processes. Role and review of the determination methods of reactive oxygen species, *J. Chem. Technol. Biotechnol.*, 90 (2015) 796–820.
- [58] D.A. Coledam, M.M.S. Pupo, B.F. Silva, A.J. Silva, K.I.B. Eguiluz, G.R. Salazar-Banda, J.M. Aquino, Electrochemical mineralization of cephalexin using a conductive diamond anode: a mechanistic and toxicity investigation, *Chemosphere*, 168 (2017) 638–647.
- [59] V.T. Gawande, K.G. Bothara, A.M. Marathe, Stress studies and identification of degradation products of cephalexin using LC–PDA and LC–MS/MS, *Chromatographia*, 80 (2017) 1545–1552.
- [60] O.R.S. da Rocha, R.F. Dantas, W.J. do Nascimento Júnior, Y. Fujiwara, M.M.M.B. Duarte, J.P. da Silva, Kinetic study and modelling of cephalexin removal from aqueous solution by advanced oxidation processes through artificial neural networks, *Desal. Water Treat.*, 92 (2017) 72–79.
- [61] M.R. Samarghandi, A.R. Rahmani, M.T. Samadi, M. Kiamanesh, G. Azarian, Degradation of pentachlorophenol in aqueous solution by the UV/ZrO₂/H₂O₂ photocatalytic process, *Avicenna J. Environ. Health Eng.*, 2 (2015) 4761–4761.
- [62] S.G. Michael, I. Michael-Kordatou, S. Nahim-Granados, M.I. Polo-López, J. Rocha, A.B. Martínez-Piernas, P. Fernández-Ibáñez, A. Agüera, C.M. Manaia, D. Fatta-Kassinos, Investigating the impact of UV-C/H₂O₂ and sunlight/H₂O₂ on the removal of antibiotics, antibiotic resistance determinants and toxicity present in urban wastewater, *Chem. Eng. J.*, 388 (2020) 124383.
- [63] X.H. Liu, Y. Liu, S.Y. Lu, Z. Wang, Y.Q. Wang, G.D. Zhang, X.C. Guo, W. Guo, T.T. Zhang, B.D. Xi, Degradation difference of ofloxacin and levofloxacin by UV/H₂O₂ and UV/PS (persulfate): efficiency, factors and mechanism, *Chem. Eng. J.*, 385 (2020) 123987.
- [64] Y.W. Pan, Y. Zhang, M.H. Zhou, J.J. Cai, Y. Tian, Enhanced removal of antibiotics from secondary wastewater effluents by novel UV/pre-magnetized Fe⁰/H₂O₂ process, *Water Res.*, 153 (2019) 144–159.
- [65] H. Godini, A. Sheikhmohammadi, L. Abbaspour, R. Heydari, G.S. Khorramabadi, M. Sardar, Z. Mahmoudi, Energy consumption and photochemical degradation of Imipenem/Cilastatin antibiotic by process of UVC/Fe²⁺/H₂O₂ through response surface methodology, *Optik*, 182 (2019) 1194–1203.
- [66] Q. Jiang, R.L. Zhu, Y.P. Zhu, Q.Z. Chen, Efficient degradation of cefotaxime by a UV+ferrihydrite/TiO₂+H₂O₂ process: the important role of ferrihydrite in transferring photo-generated electrons from TiO₂ to H₂O₂, *J. Chem. Technol. Biotechnol.*, 94 (2019) 2512–2521.
- [67] R.C. Zhang, Y.K. Yang, C.-H. Huang, L. Zhao, P.Z. Sun, Kinetics and modeling of sulfonamide antibiotic degradation in wastewater and human urine by UV/H₂O₂ and UV/PDS, *Water Res.*, 103 (2016) 283–292.